coatings

MDPI

Article

Humic Acid Removal in Water via UV Activated Sodium Perborate Process

Deling Yuan [1,2], Zhihui Zhai [1], Eryu Zhu [1], Huilin Liu [1], Tifeng Jiao [1,2,*] and Shoufeng Tang [1,2,*]

[1] Hebei Key Laboratory of Heavy Metal Deep-Remediation in Water and Resource Reuse, Hebei Key Laboratory of Applied Chemistry, School of Environmental and Chemical Engineering, Yanshan University, Qinhuangdao 066004, China; yuandl@ysu.edu.cn (D.Y.); zzhdyx06@163.com (Z.Z.); zhueryu2022@163.com (E.Z.); liuhl0094@163.com (H.L.)

[2] State Key Laboratory of Metastable Materials Science and Technology, Yanshan University, Qinhuangdao 066004, China

* Correspondence: tfjiao@ysu.edu.cn (T.J.); tangshf@ysu.edu.cn (S.T.)

Abstract: Humic acid (HA) has complex molecular structure and is capable of adsorption, ion exchange, and chelation with organic and inorganic pollutants in water bodies, worsening water quality and jeopardizing human health and ecological environment. How to effectively remove HA from water is one of the research focuses of this paper. In this study, the UV-activated sodium perborate (SPB) synergistic system (UV/SPB) was established to eliminate HA in water. The effects of initial HA concentration, SPB dose, and initial pH value on the HA elimination were determined, and the main mechanisms of the synergy and HA degradation were explored. The outcomes show that the HA elimination ratio by the sole UV and only SPB system were only 0.5% and 1.5%, respectively. The HA removal of UV/SPB reached 88.8%, which can remove HA more effectively than other systems. Free radical masking experiment proved that hydroxyl radical produced by SPB activation is the main active substance for HA removal. The results of UV-vis absorption spectrum, absorbance ratio, specific UV absorbance, and excitation–emission matrix spectroscopy verified that the UV/SPB system can effectively decompose and mineralize HA.

Keywords: UV irradiation; sodium perborate; activation; humic acid removal; decomposition mechanism

Citation: Yuan, D.; Zhai, Z.; Zhu, E.; Liu, H.; Jiao, T.; Tang, S. Humic Acid Removal in Water via UV Activated Sodium Perborate Process. *Coatings* **2022**, *12*, 885. https://doi.org/10.3390/coatings12070885

Academic Editor: Ioannis V. Yentekakis

Received: 18 May 2022
Accepted: 21 June 2022
Published: 22 June 2022

1. Introduction

As a non-uniform macromolecular polymer, humic acid (HA) is the major ingredient of natural organic matter (NOM), which is the product of polymerization of diverse biologic remains for ages [1]. HA has a complex molecular structure and contains many organic functional groups, such as hydroxyl, carboxyl, carbonyl, methoxy, and quinone groups, which are capable of adsorption, ion exchange, and chelation with organic and inorganic pollutants in water bodies, worsening water quality and jeopardizing human health and ecological environment [2]. Finding a proper way to effectively remove HA from water is one of the focuses in environmental research.

The main methods for controlling HA in water are physical and chemical oxidation ways. Physical methods to remove HA include coagulation [3], flocculation [4], and adsorption [5], but these methods only transfer HA to solid phase, and subsequent solid waste treatment is still required. Chemical oxidation is of great interest because of its rapid decomposition and mineralization for HA [6]. Photocatalysis [7–9], Fenton oxidation [10], and electrochemical oxidation [11] are the common chemical oxidation methods for organic wastewater treatment; however, they universally have some shortcomings such as harsh reaction conditions and complex operation.

Sodium perborate (SPB, $NaBO_3$) is a widely used in situ oxidizing agent. Distinct from the sodium percarbonate, SPB is not an adduct from inorganic salt and H_2O_2 but contains cyclic perborate ions ($B_2O_8H_4^{2-}$) consisting of two peroxide chains without BO_3^-

ions [12]. SPB produces H_2O_2 stably after SPB is dissolved in water, so it is a good substitute for H_2O_2 [13]. Compared with liquid H_2O_2, the solid SPB is safe and easy to store and transport. Most importantly, the activation of SPB can form hydroxyl radicals (·OH) over a wide range. Ultraviolet (UV) radiation [14] and transition metal ions [15] are the main approaches for SPB activation. Researchers have used UV-activated perborate for organic pollutant removal [13]. Besides, the perborate has been employed as the oxidant in the homogeneous photo-Fenton and heterogeneous Fenton-like reactions for dye and phenol degradation [12,16], respectively. Among them, the UV activation method is easy operation and safe without secondary pollution, so it could efficaciously excite H_2O_2 to decompose organics from wastewater [17,18].

Although the UV-activated peroxide and even UV-activated SPB method have been applied for removing organics in water, the elimination of HA through the UV activated SPB is rarely reported. Therefore, the importance of this study was establishing a UV/SPB synergistic system (UV/SPB) for the reduction of HA in water. With the convenient and efficient spectrophotometric method [19], the effects of initial HA concentration, SPB dose, and initial pH value on HA decontamination were studied. The main active substances generated in the synergistic system for HA removal were determined by free radical masking experiment, and the degradation mechanism was systematically explored by UV spectra, total organic carbon, and three-dimensional excitation-emission matrix spectroscopy (3D-EEM).

2. Experimental

2.1. Chemicals

HA was purchased from Aladdin Industrial Co., Shanghai, China. The average molecular weight of HA was 2485 Da. Sodium perborate ($NaBO_3$, SPB) and sodium sulfate (Na_2SO_4) were also purchased from Aladdin Industrial Co., Shanghai, China. Sodium hydroxide (NaOH) and sulfuric acid (H_2SO_4) were purchased from Sinopharm Chemical Reagent Co., Shanghai, China. Sodium carbonate (Na_2CO_3) and sodium dihydrogen phosphate (NaH_2PO_4) were bought from Tianjin Kemiou Chemical Reagent Co., Ltd., Tianjin, China. Sodium nitrate ($NaNO_3$) was manufactured by Tianjin Hengxing Chemical Reagent Manufacturing Co., Ltd., Tianjin, China. Sodium bicarbonate ($NaHCO_3$) was supplied by Tianjin Kaitong Chemical Reagent Co., Ltd., Tianjin, China. Sodium chloride (NaCl) was obtained from Tianjin Fengchuan Chemical Reagent Co., Ltd., Tianjin, China. Tertiary butanol (TBA) was purchased from Tianjin Damao Chemical Reagent Factory, Tianjin, China. All chemicals used were of analytical grade without further purification.

2.2. Experimental Procedures

The HA removal experiments were conducted in 25 °C. A beaker served as the reactor was kept on the magnetic stirrer, and the UV lamp (power 16 W, wavelength 254 nm, Philips Co., Shanghai, China) was placed above the beaker with the distance 3.5 cm. The UV fluence in this study was computed to be 35.2 mJ cm^{-2} for 60 min. A certain volume of HA solution was diluted to 100 mL before the beginning of experiment. Then the SPB was introduced to the HA simulated wastewater, and the UV irradiation was begun to initiate the reaction. At specified time intervals, 2.5 mL aliquots were withdrawn for measuring the absorbance. All the experiments were performed at least two times. To confirm the generation of ·OH, TBA was used as the scavengers.

2.3. Method and Analyses

The absorbance of solution was detected through UV-vis spectrophotometer (SP-725 Shanghai Spectral Instrument Co., Ltd., Shanghai, China) with external standard method at a wavelength of 254 nm to determine the HA removal efficiency [20]. The equation was as follows:

$$\text{HA removal efficiency} = \frac{C_0 - C_t}{C_0} \times 100\% \quad (1)$$

where C_0 was the beginning HA amount, and C_t was the HA amount at the treatment time t.

The HA molecular structure variation was determined by a series of specific UV-vis adsorption spectra. The values of A_{253}, A_{203}, A_{254}, A_{436}, A_{250}, A_{365}, A_{465}, and A_{665} were determined by spectrophotometer at the wavelengths of 203 nm, 250 nm, 253 nm, 254 nm, 365 nm, 436 nm, 465 nm, and 665 nm, respectively [21]. In addition, continuous changes in absorbance of the solution at 200–800 nm were also measured to characterize the changes of HA molecular structure.

Total organic carbon (TOC) was measured by TOC analyzer (VCPH, Shimadzu, Japan). Specific UV absorbance ($SUVA_x$) was calculated with A_x and TOC [22].

$$SUVA_x = \frac{A_x}{TOC} \times 100\% \quad (2)$$

where A_x was the sample absorbance at x nm.

The 3D-EEM spectrum (FL4500, Hitachi, Tokyo, Japan) was used to explore the HA decomposition mechanism. The ranges emission and excitation wavelengths were from 280 to 550 nm and 200 to 400 nm, separately, and their corresponding slits were 10 and 5 nm, respectively.

3. Results and Discussion

3.1. Study on HA Removal by UV/SPB System

3.1.1. Comparison of HA Removal Performance during Different Systems

The removal of HA was firstly investigated in three processes, which were UV, SPB, and UV/SPB, as seen in Figure 1. The experimental conditions were as follows: HA concentration of 10 mg·L^{-1}, SPB dose of 1 mmol·L^{-1}, and initial pH 3. The HA was hardly removed, and the removal ratio was 0.5% after 60 min by the only UV process. The elimination of HA by the sole SPB process was also insignificant, and its decolorization ratio was 1.5% at 60 min. The decontamination efficiency by the UV/SPB process was 88.8%, which increased more significantly than the other two processes. Besides, with the same molecular weight of H_2O_2, the HA removal by the UV/H_2O_2 was conducted, and its elimination ratio only achieved 40.2% after 60 min. SPB is often used for in situ chemical oxidation, and SPB has the same function as H_2O_2 when SPB was dissolved in water (Equation (3)) [12]. In the sole SPB system, although H_2O_2 was generated in the system, it cannot be activated to produce ·OH, so HA was scarcely removed. In the UV/SPB system, H_2O_2 released from SPB can form ·OH after being irradiated by UV (Equation (4)) [14], which could oxidize and destroy functional groups in HA molecular structure.

$$NaBO_3 + H_2O \rightarrow NaBO_2 + H_2O_2 \quad (3)$$

$$H_2O_2 + h\nu \rightarrow 2{\cdot}OH \quad (4)$$

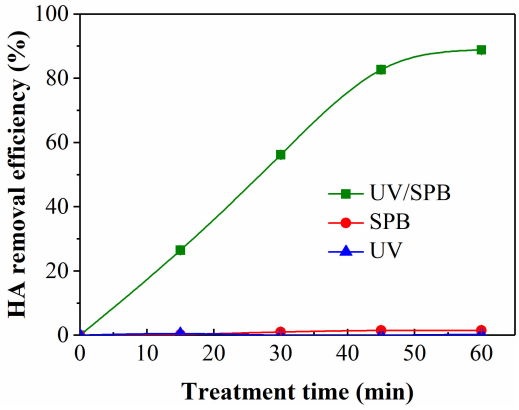

Figure 1. HA removal performance of different systems. $[HA]_0$ = 10 mg L^{-1}, $[SPB]_0$ = 1 mmol L^{-1}, pH = 3.

3.1.2. Effect of HA Concentration

The influence of HA concentration on the removal of HA by the UV/SPB system is shown in Figure 2a. The experimental conditions were SPB amount of 1 mmol L^{-1} and initial pH 3. The removal ratio decreased as the initial concentration of HA was increased. As the HA concentration was raised from 5 to 15 mg L^{-1}, the removal ration diminished from 89.8% to 70.8% after 60 min. It proved that the reactive substances formed during the UV/SPB process were persistently consumed because the active species generated in the system were insufficient to oxidize more and more contaminants in the solution, and the competition among HA molecules and reactive species became increasingly fierce with the gradual rise of HA concentration. Moreover, the HA amount enhancement would absorb more UV radiation [23], thereby inhibiting the activation of H_2O_2 and subsequently formation of ·OH radicals, which led to the decrease in HA removal.

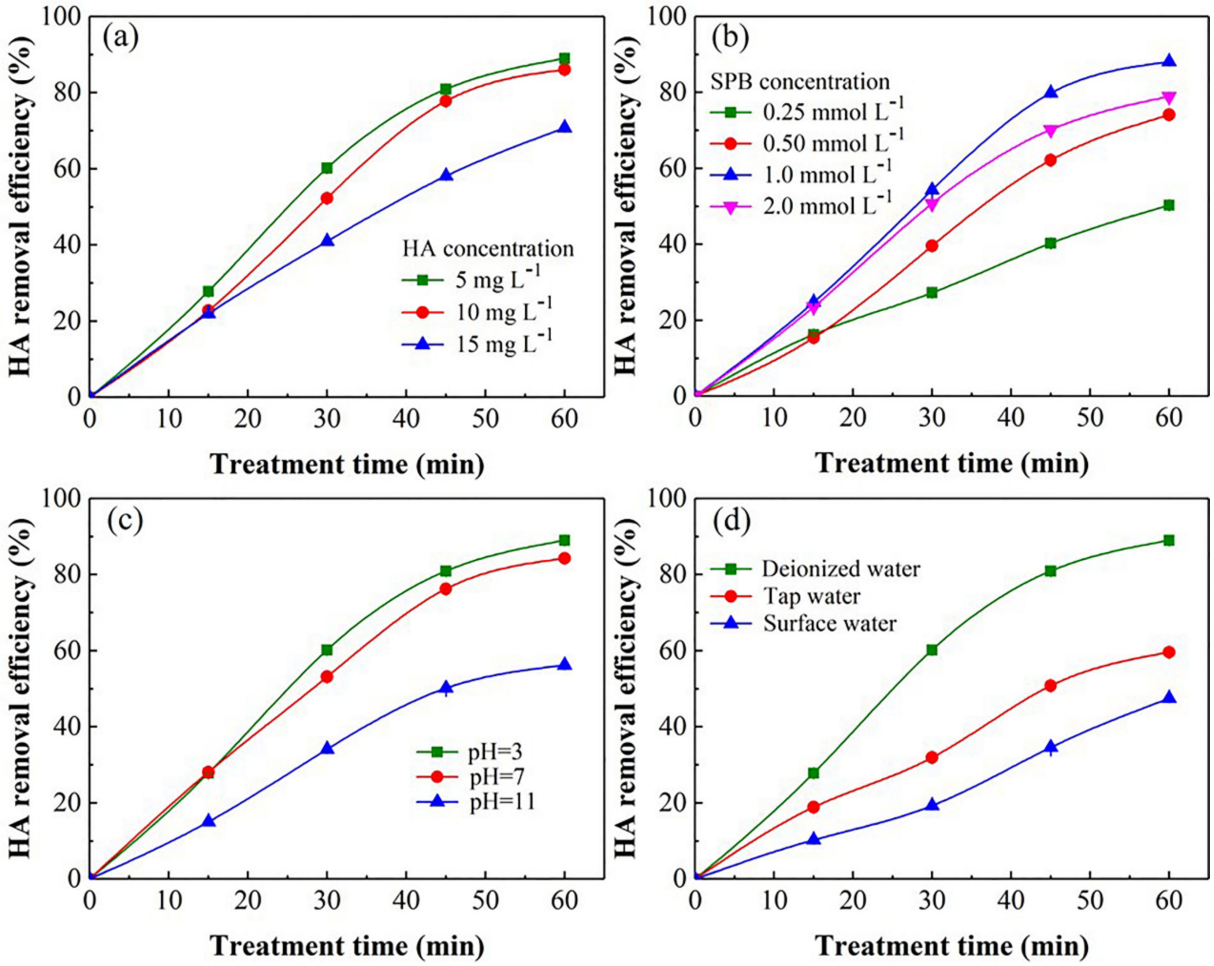

Figure 2. Influence of various parameters on HA decontamination during UV/SPB system: (**a**) HA concentration, (**b**) SPB concentration, (**c**) initial pH. ($[HA]_0$ = 5–15 mg L^{-1}, $[SPB]_0$ = 0.25–2 mmol L^{-1}, pH = 3–11). (**d**) HA removal in different waterbodies by UV/SPB. ($[HA]_0$ = 10 mg L^{-1}, $[SPB]_0$ = 1 mmol L^{-1}, pH = 3).

3.1.3. Influence of SPB Dose

The SPB is the source of active radicals which is significant for the synergetic process. The influence of SPB dosage on the HA elimination was investigated (Figure 2b). The experimental conditions were HA concentration of 10 mg L^{-1} and initial pH 3. The HA removal ratio enhanced from 53.0% to 88.8% as the SPB dosage was raised from 0.25 to 1.0 mmol L^{-1} after 60 min. With the increase of SPB concentration, the amount of active substances produced in the system was enhanced, which promoted the HA removal. However, excessive SPB would scavenge the ·OH and generate peroxy hydroxyl radical

$HO_2\cdot$ (Equation (5)) [24]. The redox potential of $HO_2\cdot$ is lower than that of ·OH. Therefore, the superfluous SPB (2.0 mmol L^{-1}) resulted in the decline of HA removal.

$$\cdot OH + H_2O_2 \rightarrow H_2O + HO_2^{\cdot} \quad (5)$$

3.1.4. Influence of Initial pH

Figure 2c shows the effect of different beginning pH on the HA removal during the UV/SPB treatment. The experimental conditions were HA concentration of 10 mg L^{-1} and SPB amount of 1 mmol L^{-1}. The HA removal decreased from 88.8% to 58.4% after 60 min while the pH value was elevated from 3 to 11. The HA molecule is neutral under strong acidic conditions, so its photochemical activity is stronger than those during neutral and basic circumstances. The redox potential $E_{\cdot OH,\ H2O}$ is also affected by pH. With the increase of pH from 3 to 11, the redox of $E_{\cdot OH,\ H2O}$ is declined from 2.62 V (pH = 3) to 2.15 V (pH = 11) [25]. Under the alkaline condition, the ·OH would be transformed to $O\cdot^-$ (E = 1.78 V) via reaction (Equation (6)) [26], which had a lower oxidation capacity than that of ·OH. As the pH increased to 11, the predominant form of H_2O_2 is changed to HO_2^-, which has a higher rate constant with ·OH ($k = 7.5 \times 10^9\ M^{-1}\ s^{-1}$, Equation (7)) than the reaction of H_2O_2 and ·OH ($k = 2.7 \times 10^7\ M^{-1}\ s^{-1}$, Equation (8)) [27], leading to the consumption of ·OH.

$$OH^- + \cdot OH \rightarrow H_2O + O^- \quad (6)$$

$$HO_2^- + \cdot OH \rightarrow OH^- + HO_2^{\cdot}\ k = 7.5 \times 10^9\ M^{-1}\ s^{-1} \quad (7)$$

$$\cdot OH + H_2O_2 \rightarrow H_2O + HO_2^{\cdot}\ k = 2.7 \times 10^7\ M^{-1} \quad (8)$$

3.1.5. HA Removal in Different Water Bodies

Figure 2d indicates the HA removal in various water bodies by the UV/SPB system. After 60 min reaction, the removal ratios of HA during deionized water, tap water, and lake water were 88.8%, 59.6%, and 47.5%, separately. It showed that the lake water and tap water inhibited the removal of HA. The reasons were as follows. Firstly, the other NOM in lake would compete with ·OH generated by UV/SPB. Secondly, the presence of various anions in the lake water and tap water that could inhibit the activity of the oxidative species, leading to a lower efficiency of HA elimination.

3.1.6. Effect of Common Anions in Water

Figure 3 demonstrates the effect of common anions such as CO_3^{2-}, HCO_3^-, Cl^-, NO_3^-, SO_4^{2-}, and $H_2PO_4^-$ for the HA elimination by the UV/SPB. In Figure 3a, when the CO_3^{2-} amount was increased from 1 to 10 mmol L^{-1}, the removal efficiency decreased from 63.7% to 44.9%. The reason was that ·OH yielded in the system was consumed by CO_3^{2-} to produce $CO_3\cdot^-$ with weak oxidation capacity (Equation (9)) [28], leading to the decrease of HA removal.

$$OH\cdot + CO_3^{2-} \rightarrow CO_3^{\cdot -} + OH^- \qquad k = 4.2 \times 10^8\ M^{-1}\cdot s^{-1} \quad (9)$$

As shown in Figure 3b, with the increase of HCO_3^- concentration (1 to 10 mmol L^{-1}), the HA elimination efficiency decreased gradually (74.2% to 53.5%) at 60 min. HCO_3^- also consumed ·OH produced in the system (Equation (10)). Besides, the solution pH would be increased after the HCO_3^- addition [29].

$$\cdot OH + HCO_3^- \rightarrow H_2O + CO_3^{\cdot -}\ k = 4.2 \times 10^8\ M^{-1}\cdot s^{-1} \quad (10)$$

In Figure 3c, as the Cl^- was enhanced from 1 to 30 mmol L^{-1}, the removal of HA decreased from 84.1% to 79.9%. Excessive Cl^- would consume ·OH and form chlorine

species (Equations (11) and (12)). The reduction in oxidation capacity led to a slight decrease in HA removal [30].

$$OH\cdot + Cl^- \rightarrow ClOH^{\cdot -} \quad k = 4.3 \times 10^9\ M^{-1}\cdot s^{-1} \tag{11}$$

$$Cl^- + Cl^- \rightarrow Cl_2^{\cdot -} \quad k = 8 \times 10^9\ M^{-1}\cdot s^{-1} \tag{12}$$

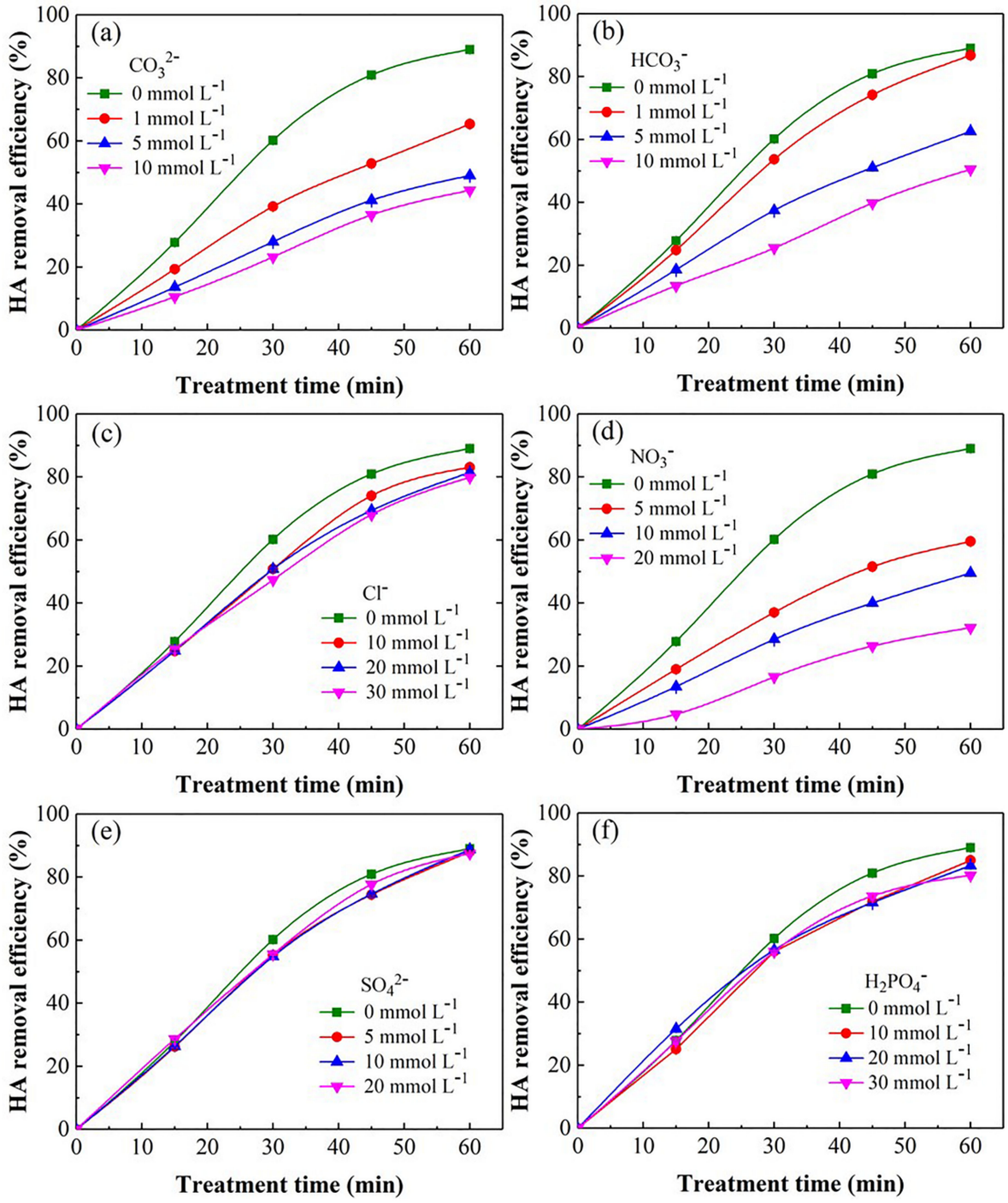

Figure 3. Effect of common anions on HA elimination in UV/SPB: (**a**) CO_3^{2-}, (**b**) HCO_3^-, (**c**) Cl^-, (**d**) NO_3^-, (**e**) SO_4^{2-}, (**f**) $H_2PO_4^-$. ($[HA]_0$ = 10 mg L^{-1}, $[SPB]_0$ = 1 mmol L^{-1}, pH = 3).

The more greater the addition of NO_3^-, the lower HA removal ratio was observed in Figure 3d. While 20 mmol L^{-1} NO_3^- was added, the HA removal was decreased to 33.4%. UV activated NO_3^- can yield free radical NO_2· (E_0 = 0.867 V), which has lower oxidation ability and would be annihilated during the UV/SPB (Equations (13)–(15)) [31]. In addition, NO_3^- could also directly consume ·OH (Equation (16)) [32].

$$NO_3^- + h\nu \rightarrow NO_2^{\cdot} + O^{\cdot -} \quad (13)$$

$$NO_3^- + h\nu \rightarrow NO_2^- + O \quad (14)$$

$$2NO_2^{\cdot} + H_2O \rightarrow NO_3^- + NO_2^- + 2H^+ \quad (15)$$

$$\cdot OH + NO_3^- \rightarrow NO_3^{\cdot} + OH^- \; k = 4.0 \times 10^5 \; M^{-1} \cdot s^{-1} \quad (16)$$

Figure 3e shows that the increase in SO_4^{2-} concentration did not affect the HA removal effect. When the SO_4^{2-} dosage enhanced to 20 mmol L^{-1}, the HA removal efficiency could reach 88.0%. According to the literature, SO_4^{2-} does not react with active species generated in the system [33,34], so it does not affect the HA removal remarkably.

As presented in Figure 3f, the HA elimination changed insignificantly with the addition of $H_2PO_4^-$. When the $H_2PO_4^-$ amount enhanced from 10 to 30 mmol L^{-1}, the HA elimination efficiencies were diminished from 86.3% to 82.4%. Although $H_2PO_4^-$ can react with ·OH· to form hydrogen phosphate radical ($HPO_4^{\cdot -}$) (Equation (17)) [35], the reaction rate is too low, which could not obviously impact the HA removal.

$$\cdot OH + H_2PO_4^- \rightarrow HPO_4^{\cdot -} + H_2O \; k = 2 \times 10^4 \; M^{-1} \cdot s^{-1} \quad (17)$$

3.2. Mechanism of HA Removal by UV/SPB

3.2.1. Scavenging Test

TBA could scavenge ·OH during oxidation process ($k_{TBA,\cdot OH}$ = 3.8–7.6 × 10^8 $M^{-1} \cdot s^{-1}$) [36]. Figure 4 demonstrates the influence of TBA addition on the HA removal in the UV/SPB. The experimental conditions were HA concentration of 10 mg L^{-1}, SPB dose of 1 mmol L^{-1}, and initial pH 3. As can be seen from the figure, adding TBA obviously restrained the HA elimination, which diminished from 16.5% to 11.5% with the addition of TBA enhanced from 0.05 to 0.5 mol L^{-1}. It testified that the main oxidizing species in the synergistic system could be ·OH. The elimination of HA was not completely inhibited after adding TBA, and this could be due to the fact that HO_2· produced by decomposition of H_2O_2 could also generate other reactive radicals, such as superoxide anion radicals ($O_2^{\cdot -}$) and single oxygen ($^1O_2$) (Equations (18)–(22)) [37,38], which also have a certain oxidation capacity and cannot be entirely suppressed by TBA.

$$H_2O_2 \rightarrow 2 \cdot OH \quad (18)$$

$$\cdot OH + H_2O_2 \rightarrow HO_2^{\cdot} + H_2O \quad (19)$$

$$HO_2^{\cdot} \rightarrow O_2^{\cdot -} + H^+ \quad (20)$$

$$\cdot OH + O_2^{\cdot -} \rightarrow {}^1O_2 + OH^- \quad (21)$$

$$2O_2^{\cdot -} + 2H^+ \rightarrow {}^1O_2 + H_2O_2 \quad (22)$$

3.2.2. HA Decomposition Mechanism

The absorbance ratios (A_{253}/A_{203}, A_{250}/A_{365}, A_{254}/A_{436} and A_{465}/A_{665}) could reflect the transformation of HA molecular structure [39]. The evolution of these ratios in the UV/SPB system is shown in Figure 5a. With the increase in reaction time, the value of A_{253}/A_{203} decreased from 0.98 to 0.44, indicating that the stability of functional groups (such as carboxyl and carbonyl groups) in HA aromatic structure gradually diminished. The increase of A_{250}/A_{365} value from 2.42 to 3.20 suggested the decrease in the HA molecular weight. The A_{254}/A_{436} increased from 4.63 to 5.60, demonstrating that the HA chromophore

was destroyed. The value of A_{465}/A_{665} decreased from 3.5 to 1.0 and proved the destruction of aromaticity in HA.

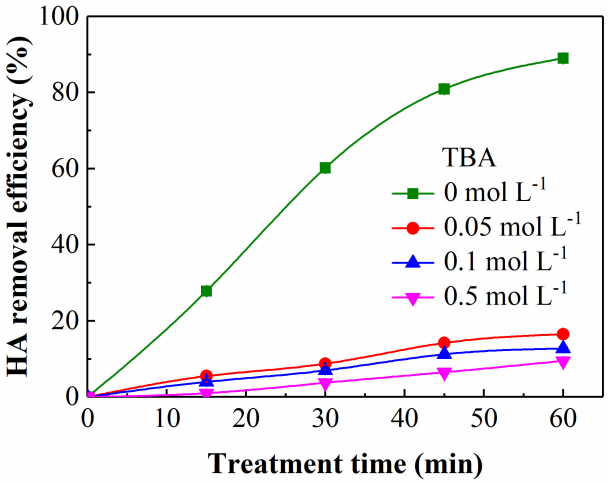

Figure 4. Influence of TBA addition on HA elimination. $[HA]_0$ = 10 mg L^{-1}, $[SPB]_0$ = 1 mmol L^{-1}, pH = 3.

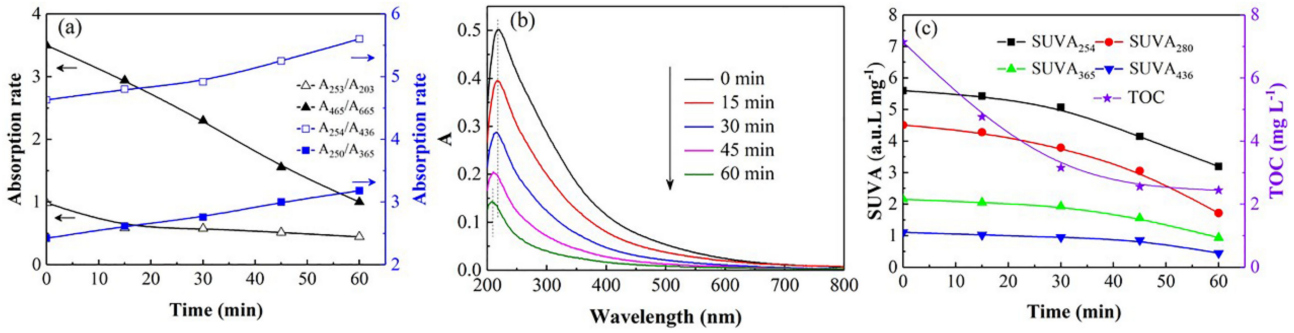

Figure 5. (**a**) UV absorption rate; (**b**) UV-vi spectrum; (**c**) $SUVA_x$ and TOC concentration for HA decomposition. $[HA]_0$ = 10 mg L^{-1}, $[SPB]_0$ = 1 mmol L^{-1}, pH = 3.

The UV-visible absorption spectrum can also manifest the changes of HA molecular structure. Figure 5b shows that the variation of the absorption spectrum of HA in the UV/SPB system over time. The absorption peak of HA at 200–250 nm weakened over time, indicating that ·OH generated in the UV/SPB system destroyed the chromophore groups and double bond structure of HA, and the unsaturated ketone was also oxidized. Moreover, the absorption peak moved to the direction of short wavelength, which was the phenomenon of blue shift. This demonstrated that the substitution reaction of a carbon atom occurred at the carbonylic group in the HA chromophore [40]. HA and fulvic acid are composed of linearly thickened aromatic rings and unsaturated carbons. When the carbon atom of chromophore, such as carbonyl, is substituted by some substituent groups, the absorption peak would shift to the short wavelength [41].

Specific ultraviolet absorbances ($SUVA_{254}$, $SUVA_{280}$, $SUVA_{365}$, and $SUVA_{436}$) were generally selected to characterize the degradation and mineralization for NOM. $SUVA_{254}$ reflects the molecular weight, $SUVA_{280}$ corresponds to the integrity of aromatic structure, $SUVA_{365}$ indicates the molecular volume, and $SUVA_{436}$ represents the chromophore situation in NOM [39]. It can be seen from Figure 5c that the decrease in the $SUVA_{254}$ and $SUVA_{280}$ values over time demonstrated that the molecular weight of organic compounds diminished, and the original aromatic structure was destructed after 60 min treatment in the UV/SPB. The decline of $SUVA_{365}$ indicated that the volume of organic molecules reduced as the reaction progressed. The decreasing value of $SUVA_{436}$ proved that the functional groups and chromophores were destructed by various reactive species. In addition, TOC

in the system was lessened from 7.139 to 2.440 mg L^{-1}, and the mineralization efficiency reached 65.8%, demonstrating that most of HA had been mineralized into H_2O and CO_2. The results of UV spectrum and TOC proved that the UV/SPB synergistic treatment can effectively decompose the complex molecular structure of HA.

3D-EEM was used to further explore the degradation mechanism of HA in the UV/SPB system, and the results are shown in Figure 6. The scanning spectrum was divided into five regions because of the complexity of spectral response and scanning sample. The range of I and II can represent aromatic proteins in organic compounds which related to the structure of aromatic ring amino acids in NOM [42]. III region indicates fulminate-like substances related to hydroxyl and carboxyl groups in the humus structure. The range of region IV corresponds to the small molecular structure of organic matter [35]. The V region indicates to humic-like fluorescence [42,43]. It is clear that the fluorescence intensity of the five regions all diminished and gradually disappeared from 0 min (Figure 6a) to 15 min (Figure 6b) and 60 min (Figure 6c), which further proved that the HA molecular structure was decomposed and mineralized in this collaborative system.

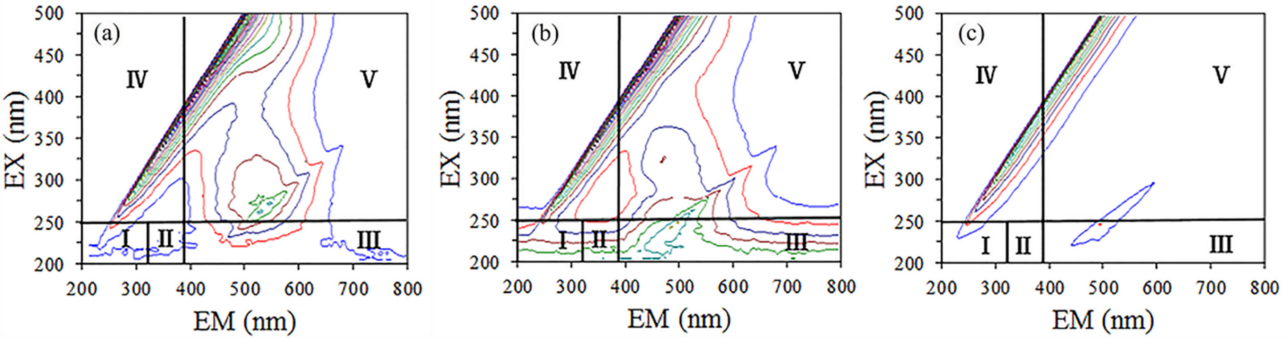

Figure 6. Time-varying 3D-EEM spectra of HA in UV/SPB system. (**a**) 0 min, (**b**) 15 min, (**c**) 60 min.

4. Conclusions

In this study, the UV/SPB synergistic system was established to remove HA from water, and the experimental results demonstrated that the UV/SPB process can effectively decompose HA. Under the experimental conditions of 10 mg L^{-1} HA concentration, 1 mmol L^{-1} SPB dosage, and beginning pH 3, the HA removal efficiency reached 88.8% after 60 min treatment. The HA removals in lake water and tap water were significantly lower than that in deionized water. The anion effect experiments confirmed that except for Cl^-, SO_4^{2-}, and $H_2PO_4^-$, the CO_3^{2-}, HCO_3^-, and NO_3^- inhibited the removal of HA to different degrees. The ·OH generated by SPB activation was suggested to be the main active substance for HA removal by masking experiments. The results of UV-vis spectrum, absorbance ratio, specific ultraviolet absorbance, and 3D-EEM jointly proved that the synergistic system could effectively degrade and mineralize HA in water.

Author Contributions: Conceptualization, D.Y. and S.T.; writing—review and editing, D.Y.; writing—original draft preparation, Z.Z.; investigation, E.Z. and H.L.; supervision, T.J.; project administration, S.T.; funding acquisition, D.Y. and S.T. All authors have read and agreed to the published version of the manuscript.

Funding: The authors acknowledge the Central Guidance on Local Science and Technology Development Fund of Hebei Province (No. 226Z3603G), the Natural Science Foundation of Hebei province (Nos. E2020203185, B2020203033), the Hebei Province Foundation for Returnees (No. C20210502), and the University Science and Technology Program Project of Hebei Provincial Department of Education (No. QN2020143).

Institutional Review Board Statement: Not applicable.

Informed Consent Statement: Not applicable.

Data Availability Statement: Not applicable.

Conflicts of Interest: The authors declare no conflict of interest.

References

1. Ryu, J.; Jung, J.; Park, K.; Song, W.; Choi, B.; Kweon, J. Humic acid removal and microbial community function in membrane bioreactor. *J. Hazard. Mater.* **2021**, *417*, 126088. [CrossRef] [PubMed]
2. Cui, L.; Zhang, Y.; He, K.; Sun, M.; Zhang, Z. Ti4O7 reactive electrochemical membrane for humic acid removal: Insights of electrosorption and electrooxidation. *Sep. Purif. Technol.* **2022**, *293*, 121112. [CrossRef]
3. Yue, Y.; An, G.; Lin, L.; Demissie, H.; Yang, X.; Jiao, R.; Wang, D. Design and coagulation mechanism of a new functional composite coagulant in removing humic acid. *Sep. Purif. Technol.* **2022**, *292*, 121016. [CrossRef]
4. Huang, X.; Wan, Y.; Shi, B.; Shi, J. Effects of powdered activated carbon on the coagulation-flocculation process in humic acid and humic acid-kaolin water treatment. *Chemosphere* **2019**, *238*, 124637. [CrossRef]
5. Chen, Y.; Qian, Y.; Ma, J.; Mao, M.; Qian, L.; An, D. New insights into the cooperative adsorption behavior of Cr(VI) and humic acid in water by powdered activated carbon. *Sci. Total Environ.* **2022**, *817*, 153081. [CrossRef] [PubMed]
6. Lee, S.; Roh, Y.; Koh, D.-C. Oxidation and reduction of redox-sensitive elements in the presence of humic substances in subsurface environments: A review. *Chemosphere* **2018**, *220*, 86–97. [CrossRef] [PubMed]
7. Oskoei, V.; Dehghani, M.H.; Nazmara, S.; Heibati, B.; Asif, M.; Tyagi, I.; Agarwal, S.; Gupta, V.K. Removal of humic acid from aqueous solution using UV/ZnO nano-photocatalysis and adsorption. *J. Mol. Liq.* **2015**, *213*, 374–380. [CrossRef]
8. Doustkhah, E.; Esmat, M.; Fukata, N.; Ide, Y.; Hanaor, D.A.; Assadi, M.H.N. MOF-derived nanocrystalline ZnO with controlled orientation and photocatalytic activity. *Chemosphere* **2022**, *303*, 124932. [CrossRef]
9. Hashemzadeh, B.; Alamgholiloo, H.; Pesyan, N.N.; Asgari, E.; Sheikhmohammadi, A.; Yeganeh, J.; Hashemzadeh, H. Degradation of ciprofloxacin using hematite/MOF nanocomposite as a heterogeneous Fenton-like catalyst: A comparison of composite and core−shell structures. *Chemosphere* **2021**, *281*, 130970. [CrossRef]
10. Huang, B.; Qi, C.; Yang, Z.; Guo, Q.; Chen, W.; Zeng, G.; Lei, C. Pd/Fe3O4 nanocatalysts for highly effective and simultaneous removal of humic acids and Cr(VI) by electro-Fenton with H2O2 in situ electro-generated on the catalyst surface. *J. Catal.* **2017**, *352*, 337–350. [CrossRef]
11. Maqbool, T.; Ly, Q.V.; He, K.; Cui, L.; Zhang, Y.; Sun, M.; Zhang, Z. Reactive electrochemical ceramic membrane for effective removal of high concentration humic acid: Insights of different performance and mechanisms. *J. Membr. Sci.* **2022**, *651*, 120460. [CrossRef]
12. Zhang, C.; Dong, Y.; Li, B.; Li, F. Comparative study of three solid oxidants as substitutes of H2O2 used in Fe (III)-oxalate complex mediated Fenton system for photocatalytic elimination of reactive azo dye. *J. Clean. Prod.* **2018**, *177*, 245–253. [CrossRef]
13. Sindelar, H.R.; Brown, M.T.; Boyer, T.H. Evaluating UV/H2O2, UV/percarbonate, and UV/perborate for natural organic matter reduction from alternative water sources. *Chemosphere* **2014**, *105*, 112–118. [CrossRef]
14. Gao, J.; Song, J.; Ye, J.; Duan, X.; Dionysiou, D.D.; Yadav, J.S.; Nadagouda, M.N.; Yang, L.; Luo, S. Comparative toxicity reduction potential of UV/sodium percarbonate and UV/hydrogen peroxide treatments for bisphenol A in water: An integrated analysis using chemical, computational, biological, and metabolomic approaches. *Water Res.* **2020**, *190*, 116755. [CrossRef]
15. Habibi, D.; Zolfigol, M.A.; Safaiee, M.; Shamsian, A.; Ghorbani-Choghamarani, A. Catalytic oxidation of sulfides to sulfoxides using sodium perborate and/or sodium percarbonate and silica sulfuric acid in the presence of KBr. *Catal. Commun.* **2009**, *10*, 1257–1260. [CrossRef]
16. LACSA, F. Oxidative Degradation of Phenol via Heterogeneous Fenton-Like Reaction over Fe-ZSM5 Catalyst Using Sodium Perborate and Sodium Percarbonate as Oxidants. Ph.D. Thesis, Ateneo de Manila University, Metro Manila, Philippines, 2017.
17. Chang, X.; Lin, T.; Mo, J.; Xu, H.; Tao, H.; Liu, W. Coagulation combined with ultraviolet irradiation activated sodium percarbonate as pretreatment prior to ultrafiltration: Analysis of free radical oxidation mechanism and membrane fouling control. *Chemosphere* **2022**, *287*, 132049. [CrossRef]
18. Gao, J.; Nunes, R.F.; O'Shea, K.; Saylor, G.L.; Bu, L.; Kang, Y.-G.; Duan, X.; Dionysiou, D.D.; Luo, S. UV/Sodium percarbonate for bisphenol A treatment in water: Impact of water quality parameters on the formation of reactive radicals. *Water Res.* **2022**, *219*, 118457. [CrossRef]
19. Alminshid, A.H.; Alalwan, H.A.; Abdulghani, H.A.; Mohammed, M.M. Spectrophotometric study of ephedrine hydrochloride in drug using molecular absorption UV–Visible. Spectrochim. *Acta Part A Mol. Biomol. Spectrosc.* **2022**, *270*, 120828. [CrossRef]
20. Zhou, X.-F.; Liang, J.-P.; Zhao, Z.-L.; Yuan, H.; Qiao, J.-J.; Xu, Q.-N.; Wang, H.-L.; Wang, W.-C.; Yang, D.-Z. Ultra-high synergetic intensity for humic acid removal by coupling bubble discharge with activated carbon. *J. Hazard. Mater.* **2021**, *403*, 123626. [CrossRef]
21. Cui, Y.; Yu, J.; Su, M.; Jia, Z.; Liu, T.; Oinuma, G.; Yamauchi, T. Humic acid removal by gas–liquid interface discharge plasma: Performance, mechanism and comparison to ozonation. *Environ. Sci. Water Res. Technol.* **2019**, *5*, 152–160. [CrossRef]
22. Yuan, D.; Tang, J.; Nie, Z.; Tang, S. Study on humic acid removal in water by ultraviolet activated sodium percarbonate. *J. Yanshan Univ.* **2021**, *45*, 220–226.
23. Li, X.; Wu, B.; Zhang, Q.; Xu, D.; Liu, Y.; Ma, F.; Gu, Q.; Li, F. Mechanisms on the impacts of humic acids on persulfate/Fe2+-based groundwater remediation. *Chem. Eng. J.* **2019**, *378*, 122142. [CrossRef]
24. Tan, C.; Gao, N.; Deng, Y.; Zhang, Y.; Sui, M.; Deng, J.; Zhou, S. Degradation of antipyrine by UV, UV/H2O2 and UV/PS. *J. Hazard. Mater.* **2013**, *260*, 1008–1016. [CrossRef] [PubMed]

25. Buxton, G.V.; Greenstock, C.L.; Helman, W.P.; Ross, A.B. Critical review of rate constants for reactions of hydrated electrons, hydrogen atoms and hydroxyl radicals (OH/O) in Aqueous Solution. *J. Phys. Chem. Ref. Data* **1988**, *17*, 513–886. [CrossRef]
26. Tang, S.; Yuan, D.; Rao, Y.; Li, M.; Shi, G.; Gu, J.; Zhang, T. Percarbonate promoted antibiotic decomposition in dielectric barrier discharge plasma. *J. Hazard. Mater.* **2019**, *366*, 669–676. [CrossRef]
27. Das, D.; Bordoloi, A.; Achary, M.P.; Caldwell, D.J.; Suri, R.P. Degradation and inactivation of chromosomal and plasmid encoded resistance genes/ARBs and the impact of different matrices on UV and UV/H2O2 based advanced oxidation process. *Sci. Total Environ.* **2022**, *833*, 155205. [CrossRef]
28. Yuan, D.; Zhang, C.; Tang, S.; Wang, Z.; Sun, Q.; Zhang, X.; Jiao, T.; Zhang, Q. Ferric ion-ascorbic acid complex catalyzed calcium peroxide for organic wastewater treatment: Optimized by response surface method. *Chin. Chem. Lett.* **2021**, *32*, 3387–3392. [CrossRef]
29. Fang, J.; Fu, Y.; Shang, C. The Roles of Reactive Species in Micropollutant Degradation in the UV/Free Chlorine System. *Environ. Sci. Technol.* **2014**, *48*, 1859–1868. [CrossRef]
30. Cai, L.; Li, L.; Yu, S.; Guo, J.; Kuppers, S.; Dong, L. Formation of odorous by-products during chlorination of major amino acids in East Taihu Lake: Impacts of UV, UV/PS and UV/H2O2 pre-treatments. *Water Res.* **2019**, *162*, 427–436. [CrossRef]
31. Ji, Y.; Zeng, C.; Ferronato, C.; Chovelon, J.-M.; Yang, X. Nitrate-induced photodegradation of atenolol in aqueous solution: Kinetics, toxicity and degradation pathways. *Chemosphere* **2012**, *88*, 644–649. [CrossRef]
32. Xu, Z.; Shan, C.; Xie, B.; Liu, Y.; Pan, B. Decomplexation of Cu(II)-EDTA by UV/persulfate and UV/H2O2: Efficiency and mechanism. *Appl. Catal. B Environ.* **2017**, *200*, 439–447. [CrossRef]
33. Tang, S.; Wang, Z.; Yuan, D.; Zhang, C.; Rao, Y.; Wang, Z.; Yin, K. Ferrous ion-tartaric acid chelation promoted calcium peroxide fenton-like reactions for simulated organic wastewater treatment. *J. Clean. Prod.* **2020**, *268*, 122253. [CrossRef]
34. Yuan, D.; Yang, K.; Zhu, E.; Li, X.; Sun, M.; Xiao, L.; Hari, Q.; Tang, S. Peracetic Acid Activated with Electro-Fe2+ Process for Dye Removal in Water. *Coatings* **2022**, *12*, 466. [CrossRef]
35. Tang, S.; Tang, J.; Yuan, D.; Wang, Z.; Zhang, Y.; Rao, Y. Elimination of humic acid in water: Comparison of UV/PDS and UV/PMS. *RSC Adv.* **2020**, *10*, 17627–17634. [CrossRef]
36. Zhao, M.; Xiang, Y.; Jiao, X.; Cao, B.; Tang, S.; Zheng, Z.; Zhang, X.; Jiao, T.; Yuan, D. MoS2 co-catalysis promoted CaO2 Fenton-like process: Performance and mechanism. *Sep. Purif. Technol.* **2021**, *276*, 119289. [CrossRef]
37. Cheng, M.; Zeng, G.; Huang, D.; Lai, C.; Xu, P.; Zhang, C.; Liu, Y. Hydroxyl radicals based advanced oxidation processes (AOPs) for remediation of soils contaminated with organic compounds: A review. *Chem. Eng. J.* **2016**, *284*, 582–598. [CrossRef]
38. Xiang, Y.; Liu, H.; Zhu, E.; Yang, K.; Yuan, D.; Jiao, T.; Zhang, Q.; Tang, S. Application of inorganic materials as heterogeneous cocatalyst in Fenton/Fenton-like processes for wastewater treatment. *Sep. Purif. Technol.* **2022**, *295*, 121293. [CrossRef]
39. Wang, T.; Qu, G.; Ren, J.; Yan, Q.; Sun, Q.; Liang, D.; Hu, S. Evaluation of the potentials of humic acid removal in water by gas phase surface discharge plasma. *Water Res.* **2016**, *89*, 28–38. [CrossRef]
40. Li, Y.; Qu, G.; Zhang, L.; Wang, T.; Sun, Q.; Liang, D.; Hu, S. Humic acid removal from micro-polluted source water using gas phase surface discharge plasma at different grounding modes. *Sep. Purif. Technol.* **2017**, *180*, 36–43. [CrossRef]
41. Wang, T.; Dongli, L.; Qu, G.; Sun, Q.; Liang, D.; Hu, S.; Zhu, L. Enhanced removal of humic acid from micro-polluted source water in a surface discharge plasma system coupled with activated carbon. *Environ. Sci. Pollut. Res.* **2017**, *24*, 21591–21600. [CrossRef]
42. Sarangapani, C.; Lu, P.; Behan, P.; Bourke, P.; Cullen, P. Humic acid and trihalomethane breakdown with potential by-product formations for atmospheric air plasma water treatment. *J. Ind. Eng. Chem.* **2018**, *59*, 350–361. [CrossRef]
43. Guo, H.; Yang, H.; Huang, J.; Tong, J.; Liu, X.; Wang, Y.; Qiao, W.; Han, J. Theoretical and experimental insight into plasma-catalytic degradation of aqueous p-nitrophenol with graphene-ZnO nanoparticles. *Sep. Purif. Technol.* **2022**, *295*, 121362. [CrossRef]